The Cosmic Vacuum? Exploring Lunar Influence on Planetary Atmospheres Post-Eruption

Esther van Dijk (s2034174), Levi van Es (s2115409), Andrés Presa Villa (s3643751)

22-12-2023

Simulation and Modeling in Astrophysics (AMUSE)

MSc Astronomy, Leiden University

Abstract

It has been found that some moons contain planetary material implanted in their surfaces. In this work , we investigate how an energetic event on the planet can influence the amount of material accreted by the moon. First, we show two possible ways of simulating the hydrodynamics of planetary atmospheres within the Astrophysical MUltipurpose Software Environment (AMUSE). Our simulations show that there is a narrow window of energies where enhanced atmospheric capture can take place. Finally, we also show that the fraction of material that can get bound to the moon increases with the mass ratio between the moon and the planet. This phenomenon could have important implications for understanding the past composition of planetary atmospheres.

1 Introduction

Planets lose part of their atmospheric gases due to different escape processes. Atmospheric escape has important implications regarding the long-term habitability of planets and their observed population distribution. In this regard, several studies have invoked atmospheric escape as a possible explanation for the observed gap in the observed exoplanet radius-period distribution (Fulton et al., 2017). Another poorly investigated phenomenon is the interaction between the escaping atmosphere and a moon orbiting the planet. In this situation, some of the atoms that escape the planetary atmosphere might be preserved inside the moon's surface. This idea has been confirmed by the detection of terrestrial ions near the Moon (Poppe et al., 2016; Terada et al., 2017) and martian material on Phobos surface (Nénon et al., 2021).

In this work, we investigate if a moon can undergo enhanced capture of planetary material in the event of an energetic burst on the planet (i.e. a volcanic eruption or an asteroid collision). If a significant amount of material passes near the moon, it is possible that lunar samples contain information about the past composition of the planet its atmosphere. We consider both the case of an Earth-like planet and a Jupiter-like planet, to cover both rocky planets and gas giants. To tackle this problem, we use the Astrophysical MUltipurpose Software Environment (AMUSE) (Portegies Zwart et al., 2009). The framework for our simulations is described in section 2. We present and discuss our results in section 3. Some conclusions and future extensions of this work are given in section 5.

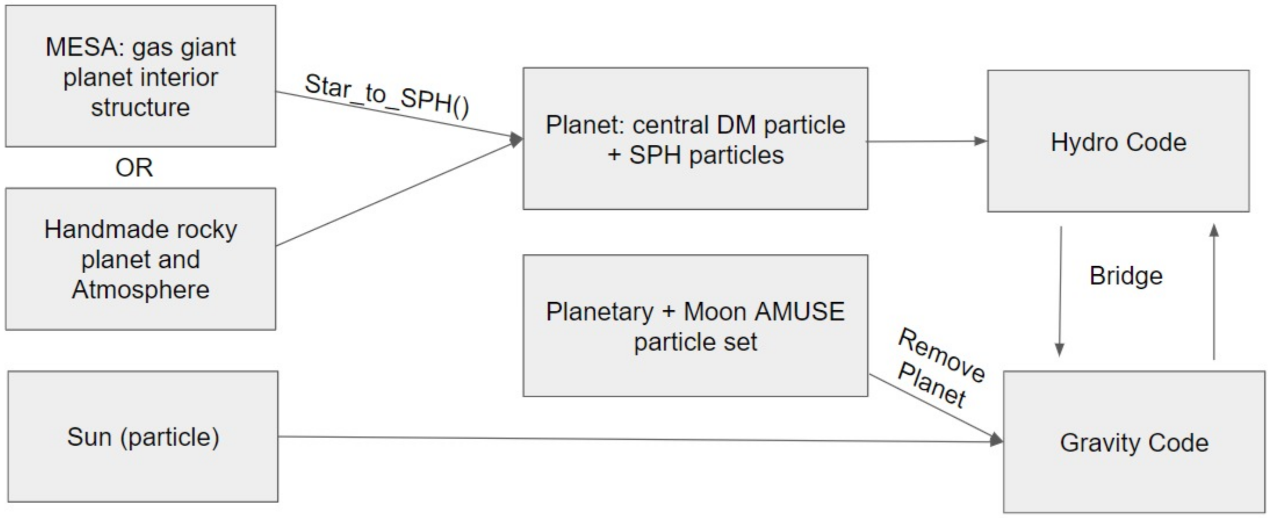

Figure 1: Schematic overview of the simulation setup.

2 Methods

The AMUSE package combines a number of simulation codes that can be combined to solve multi-physics problems. In the context of planetary physics, it has been used to model protoplanetary discs (Pelupessy & Portegies Zwart, 2013) and the evolution of gas giants (Glanz et al., 2022a), among other applications. However, it has not been used to simulate the hydrodynamics of planetary atmospheres, to our knowledge. Here, we describe the setup of our simulations and the procedures employed to create such atmospheres.

2.1 Simulation setup

In our physical setup, we combine a gravity code with a hydrodynamics code, where the planet with the atmosphere will be modelled using hydrodynamics and the moon and sun will reside in the gravity code. The hydrodynamics are in this case more important than gravity, as we want to exactly know what happens to the atmosphere when it is ejected from the planet. Requirements for our hydrodynamics code are the inclusion of an N-body code and an SPH code. This resulted in our choice for `Fi` (Hernquist & Katz, 1989). We implemented as gravity code `BHTree` (Barnes & Hut, 1986) and did not find significantly different results when experimenting with a different code. We chose to model two different types of planets: a rocky planet and a gas giant planet through different methods. These are explained in Section 2.3. Our setup is shown in Figure 1.

2.2 Constraining free variables

Effective problem-solving involves breaking down the issue into smaller, manageable parts. It's crucial to establish specific constraints to reduce the number of variables. In the fundamental model of our system, we identify six critical free variables that, when not constrained, require thorough exploration for an accurate result.

The Mass of the planet (M_p) is the first free variable in our system. We chose a combined restraint,

Variable	Rocky planet	Gas giant planet
$M_{\rm moon}/M_{\rm planet}$	0.0123	0.0515
$M_{\rm planet}(M_\oplus)$	1	388
Semi-major axis a (km)	384400	421600
eccentricity e	0	0
Atmosphere mass fraction in explosion	1	0.24
Location of the explosion	uniform	uniform
Energy of the explosion	free	free
Number of SPH particles	50000	2000
Model evolution time step (hours)	1	0.5
Model evolution duration (days)	10	4

Table 1: Constraints on the parameters in the simulation setup.

which takes not only mass of the planet into account but also the mass and orbital distance of its moon. This ensures that the system becomes a scaled analog of the earth-moon-sun system. Maintaining this ratio allows us to extrapolate the results to various-sized planets.

Several events can cause the atmosphere to be ejected from Earth. Each has its own characteristic way of doing so. The collision of an asteroid initially displaces a lot of atmosphere, launching a fraction into space. The energy released by such an impact would heat the atmosphere and potentially cause a rapid expansion, also driving some of the atmospheric gases into space. The resulting plume of atmosphere launched into space would be dependent on the **mass**, **energy**, and **location** of impact, adding another three free parameters to our system. Similarly when a volcano erupts the location and strength of the eruption also introduce the same three free parameters. To constrain these parameters we decided to isotropically insert energy throughout the entire atmosphere. This constrains the **mass** to the mass of the entire atmosphere (for the rocky planet) and a set mass fraction of the envelope for the gas giant planet and **location** to cover the entire sphere. The final constraints are summarized in Table 1. The mass of the sun is set to a solar value and the distance between the sun and planet is set to 1 AU.

2.3 Constructing the planets

In this work, we investigate the distinctive atmospheric characteristics of two classes of celestial bodies: gas planets and rocky planets. Because of the different interior structures of these two types of planets, we need a different approach to construct either planet. Our review of the literature yields very little to no information about AMUSE thin atmosphere research. This gap illustrates how difficult it will be for us to recreate this thin environment. Unlike other default functions such at `create_binary_from_orbital_elements` or `get_sun_and_planets` there is no existing function to construct a rocky planet with an atmosphere for us. This necessitates devising a custom setup within AMUSE's capabilities to accurately represent a planet with an atmosphere.

Gas planets, however, have been explored in a wider range of literature, as their interior structure can be compared to stars. AMUSE provides us with a predefined function called `star_to_sph`, which can convert an interior model produced by MESA to SPH particles.

MESA planet Approach

Modules for Experiments in Stellar Astrophysics (MESA) (Paxton et al., 2011) has mostly been used to model the interior structure and evolution of stars. However, because the interior structure equations used for stars can also be used to model gas giant planets, MESA can also be used on planets. In this scenario, the nuclear burning is zero. As a result, in literature, we can see several instances of MESA being used to model different types of (exo-)planets like sub-Neptune planets (Chen & Rogers, 2016) and gas giant planets (Glanz et al., 2022b). As such, we will use this code, which is implemented in AMUSE to model our gas giant planet.

We evolve our planet to a pre-main sequence phase to retrieve the desired interior structure, before the star would have started nuclear burning. The starting mass of the planet is 1 M_J and we evolve the planet to 0.12 Myr.

The planet needs to be converted to SPH particles to be compatible with the hydrodynamics code. We here follow the approach of de Vries et al. (2014) and replace the centre of the planet, which we are not interested in, with a single mass point (DM-particle) to reduce computing time. The module `star_to_sph.py` is used for that. The mass of this central particle, we set to 300 M_{earth}. Before we inject any energy, we evolve the model for a day to let the SPH-particles and DM-particle stabilize. Characteristics of the final planet are shown in Table 1.

Manual Approach

Planet and Atmosphere

The manual method focuses on accurately emulating a rocky planet's physical characteristics with a particular emphasis on maintaining the characteristics of a dense, rocky core while perfectly imitating a thin atmosphere. This approach can create a planet that converges to Earth's true characteristics. The model starts with a simple central SPH dark matter particle to serve as a gravitational analogue for the central planet. This DM particle contains all earth parameters such as `radius`, `mass`, `position` and `velocity`. Using the planetary properties the atmosphere is constrained to a lower and an upper boundary, setting the lowest boundary of our spherical atmospheric shell to the planetary radius and the outer boundary to this radius + 100km to account for the kármán line. The atmospheric shell is uniformly filled using a rejection sampling technique, with each particle assigned earth-like atmospheric properties based on its altitude. The choice for this earth's atmosphere profile was between different known high-resolution distributions, such as uniform, barometric and exponential distributions. After exploring all three, we established that, while not even close to approaching the distributions of other rocky planets in our solar system, it did possess the same complex gradients. To maintain a degree of these complexities we ruled out the monotonic barometric and exponential profiles. Figure 2 illustrates the temperature and density distribution retrieved from the generated atmosphere.

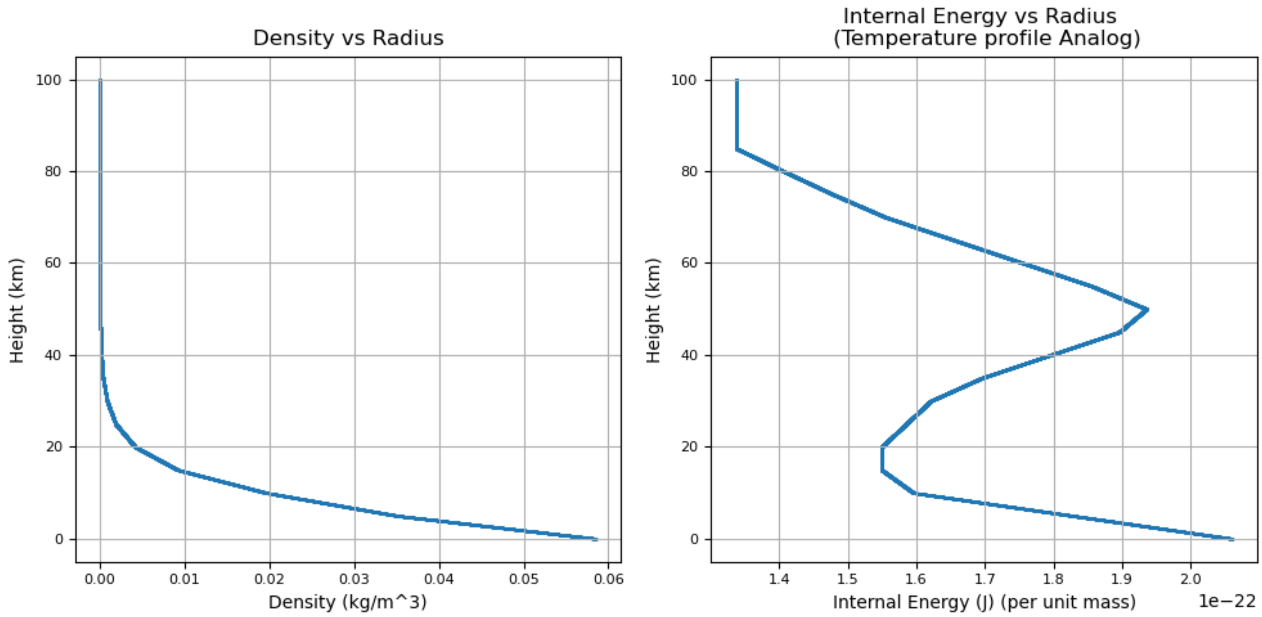

Figure 2: Atmospheric profile for

Figure 3 shows the result of combining the central DM particle with the generated atmosphere to construct the final planet.

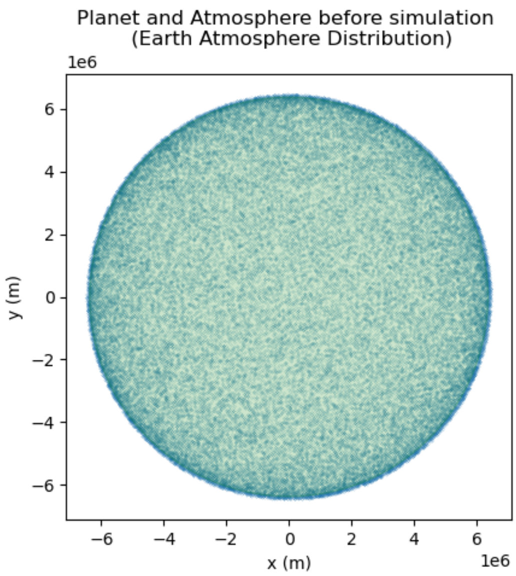

Figure 3: Central DM planet particle with barometric atmosphere

Stability

Evaluating the system's stability is crucial to ensuring both the accuracy of simulations and the system's long-term functionality. A simple method for assessing stability is to run the simulation for an extended amount of time and track any significant system changes. This approach, however, shows that our manually built system is unable to sustain stability. The crucial problem is located at the boundary between the primary "rocky" planet particle and the barometric atmosphere. Since they are both represented as hydrodynamic particles in the same simulation framework, they interact and exchange energies in the usual way that hydrodynamic particles do. Because it misrepresents the dynamics that exist between Earth's solid surface and atmosphere, this interaction is problematic.

To address this issue, we have implemented a technique in the process of injecting energy into our atmosphere. This approach is designed to eliminate hydrodynamic interactions between the centre particle and the atmosphere before the energy injection. This method ensures that the atmosphere maintains theoretical hydrostatic equilibrium at the point of energy injection, thereby maintaining a more realistic and stable simulation of the planetary system. Further details regarding energy injection are discussed in section 2.4

2.4 Simulating the explosion

MESA Approach

To simulate the explosion, we inject energy into the outer envelope of the gas planet, which equals 24% of the total mass of the envelope. This energy is distributed over the gas particles present. We use a range of energies from 1×10^{42} to 1×10^{43} erg.

Manual planet Approach

Stability has proven to be a big issue in the manual model. These stability issues are caused by planet-atmosphere interactions which disturb the atmosphere's barometric profile. To avoid these interactions we need to get the atmosphere SPH particles away from the central particle as soon as possible to avoid triggering interactions within the hydro code. This can be done by giving each particle a radial velocity equal to that of the planet's escape velocity. Velocities lower than the escape velocity would not be able to escape Earth and would not be able to reach the moon either way. These particles would then fall back onto the planet again introducing the planet-atmosphere interactions resulting in unrealistic results. Fortunately for us velocities below the escape velocity are not interesting since particles below this velocity would not be able to reach the moon either way. This puts a lower bound on the velocity of the particles in the simulations equal to the escape velocity.

Exploring the upper-bound unfortunately is less constrainable. Ultimately we aim to find the optimum velocity at which the moon can catch the most atmosphere possible. For a particle to bind to the moon, however, the particles cannot have more speed than the moon's escape velocity to get gravitationally bound. This would mean that, while the particle is very close to the moon, it is not bound and will eventually fly off and not be captured. This means that the particles must arrive at the moon with a velocity smaller than the moon's escape velocity. How the initial atmospheric velocity translates to velocity at the lunar surface unfortunately is not analytically viable to solve. This therefore requires us to explore the only free variable left from section 2.2.

The moon's escape velocity is 2.38 km/s this means that if the moon wants to capture a particle it cannot go faster than its escape velocity. We can easily finetune the ejection speed such that the speed of the atmospheric particles is below the escape velocity when it reaches the moon. Unfortunately, the moon is in orbit around the planet as well with a speed of 3.683 km/s perpendicular to the atmosphere's path. Because this velocity is perpendicular to the radial velocities of the atmospheric particles the interaction velocity between the two always has a lower limit on the relative speed of at least 3.683 km/s. This is way above the escape velocity of the moon and we would therefore not expect any atmospheric particles to bind to the planet purely gravitationally. Here we note that when the atmosphere was not ejected radially it could match the orbital speed of the moon more closely allowing for a lower relative approach velocity and therefore a higher likelihood of capture.

2.5 Calculation of the accreted atmospheric fraction

A particle will be bound to the moon if it reaches the gravitational region of influence of the moon with a sub-escape velocity. The region of gravitational influence of an object is known as the Hill sphere, and can be represented mathematically as

$$R_{Hill} \approx a(1-e)(M_{moon}/M_{planet})^{1/3}, \quad (1)$$

where a is the semi-major axis, e is the eccentricity and M_{moon} and M_{planet} are the masses of the moon and the planet, respectively. Additionally, a high velocity particle can also end on the moon if they undergo a direct collision. The resolution of our simulations depends on the likelihood of these events. The fraction of the particles that undergo a direct collision with the moon can be approximated by the ratio of the cross section of the moon and the cross section of the sphere whose radius is the semi-major axis of the moon. For the Earth-Moon system, this fraction is $f_{coll} \propto 1740^2/384000^2 \sim 10^{-5}$. To model this type of collision accurately, a resolution of millions or tens of millions of particles would be required, which is not achievable with the resources available to us here. Likewise, the probability of a particle reaching the moon with a sufficiently low velocity to be captured is also small, as particles require a high velocity to escape the planet.

In order to overcome these resolution problems, we opt for a statistical approach. Since the fraction of the ejected atmosphere captured by the moon depends on the ability of particles to reach the Hill sphere of the moon with low velocities, an order-of-magnitude estimation of this fraction can be given as:

$$f_{accreted} \sim f_{R_{Hill}} \cdot P[v = 0 \text{ within the Hill sphere}], \quad (2)$$

where $f_{R_{Hill}}$ denotes the fraction of the ejected particles that reach the Hill sphere of the moon. We can calculate this fraction from our simulations, since the resolution required to experience a significant number of particles within the Hill sphere is of no more than tens of thousands of particles. The second term in equation (2) represents the probability that a particle reaches the Hill sphere of the moon with zero velocity. We estimate this probability by fitting the velocity distribution of the particles that reach the Hill sphere to a Gaussian distribution. To ensure the Gaussian approximation holds, we perform normality hypothesis tests using the `scipy.stats.normaltest` function, and reject our model if the resulting p-value is lower than 0.2. An example of this technique is given in Figure 4.

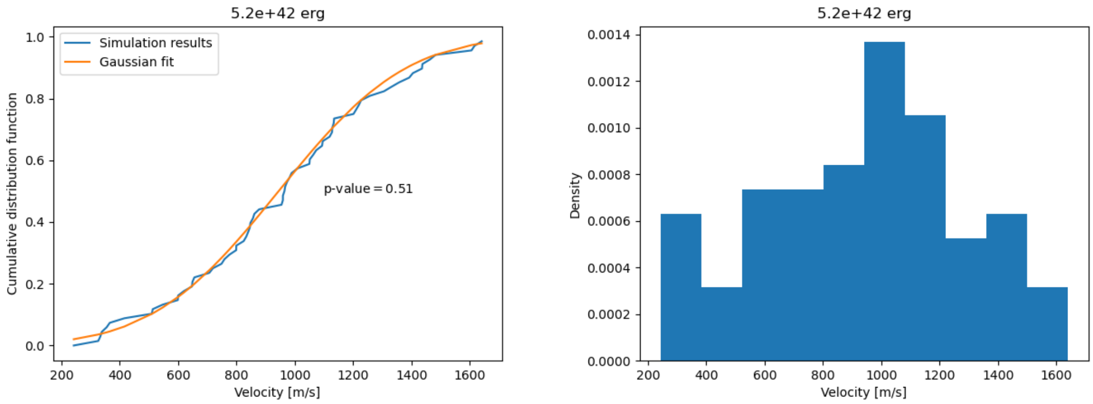

Figure 4: Velocities distribution of the particles that reach the Hill sphere of the moon. The results are shown for a gas giant and an injected energy of $5.2 \cdot 10^{42}$ erg. Left: empirical cumulative distribution function (blue) and Gaussian fit (orange). Right: empirical probability density function.

3 Results

We study two representative systems: a gas giant system and an rocky system. For the gas giant system, we consider a 1.22 Jupiter mass planet with a moon orbiting 421600 km apart from the planet. This distance is comparable to the semi-major axis of Io. We also set the mass of the moon to be around 5% of the total mass of the planet. Although this value is unrealistically large for gas giants, we adopt this value in order to ensure the Hill sphere of the moon is big enough for our low resolution simulations. Our rocky system is analogous to the Earth. A summary of both systems and the simulation can be found in table 1. We run the simulation for the different explosion energies or ejecting velocities and explore in Section 3.1 the resulting velocities of particles in the Hill sphere of the moon and show in Section 3.2 the results of the probabilistic approach explained in Section 2.5.

3.1 Velocities of gas particles in the hill sphere

To track whether a particle would theoretically get bound to the moon, we track if particles are within the hill sphere of the moon (as defined in Equation 1) and calculate some different properties. First of all, we expect the particle to be bound to the moon if the relative velocity with respect to the moon is smaller than the escape velocity from the moon. We can see in Figure 5 that this the case for both the simulation for the rocky planet and for the gas giant planet. However, we note that these particles do not stay bound in our simulation.

For the rocky planet the velocities of the particles with respect to planet are all larger than the escape velocity from the planet, which results directly from our constraints on the radial velocity of the ejecting atmosphere (see the left side of Figure 6). We find one particle, in the simulation with the ejecting velocity of 12550 m/s, that has a relative velocity with respect to the moon that is smaller than the escape velocity for the rocky planet. In the gas giant planet simulation the velocities of the particles are more distributed. A significant amount of particles have a velocity lower than the escape velocity from the planet (as visible in the right side of Figure 6), resulting in the particles bouncing back to the planet. However, the simulation with an injected energy of 3.7×10^{42} erg and 4.0×10^{42} erg show at one point in our evolution one particle in the hill sphere with a relative velocity with

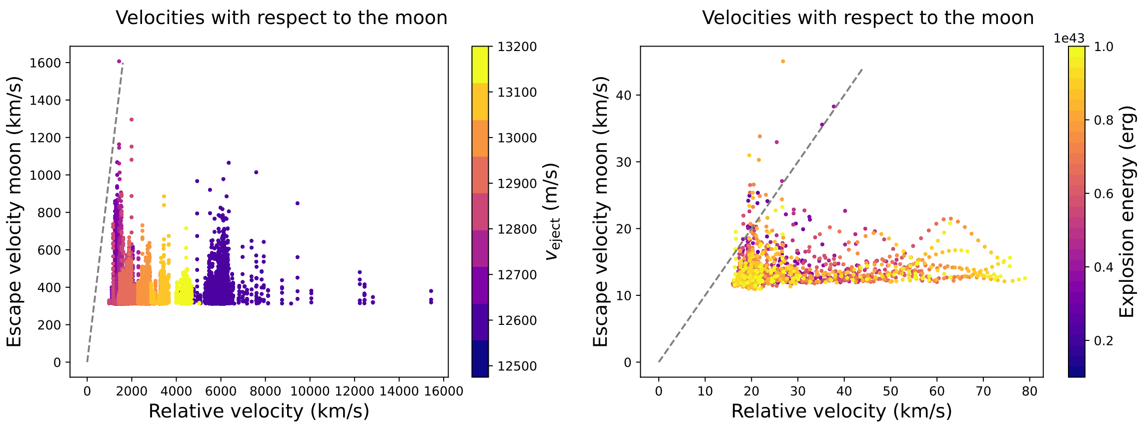

Figure 5: The left figure shows the relative velocity with respect to the moon and the escape velocity from the moon of the gas particles within the hill sphere of the moon at a certain time point in the simulation for the rocky planet. The right figure shows the same for the gas giant planet. The colours indicate the different ejecting velocities for the rocky planet and the injecting energies for the gas giant planet.

respect to the moon lower than the escape velocity of the moon and a relative velocity with respect to the planet higher than the escape velocity from the planet.

3.2 Probabilistic approach

We calculate for these simulations the fraction of the ejected atmosphere accreted by the moon following Equation (2). The results are shown in Figure 7. For both the rocky and the gas giant system, there is a small window where atmospheric capture is possible. This region is separated by a low velocity region, where we do not see any collision, and a high velocity region, where the particles are too energetic to be bound to the moon. In the high velocity region, the distribution of velocities is not Gaussian anymore, as it loses the left tail of the distribution (corresponding to low velocities). An example of this situation is given in Figure 8.

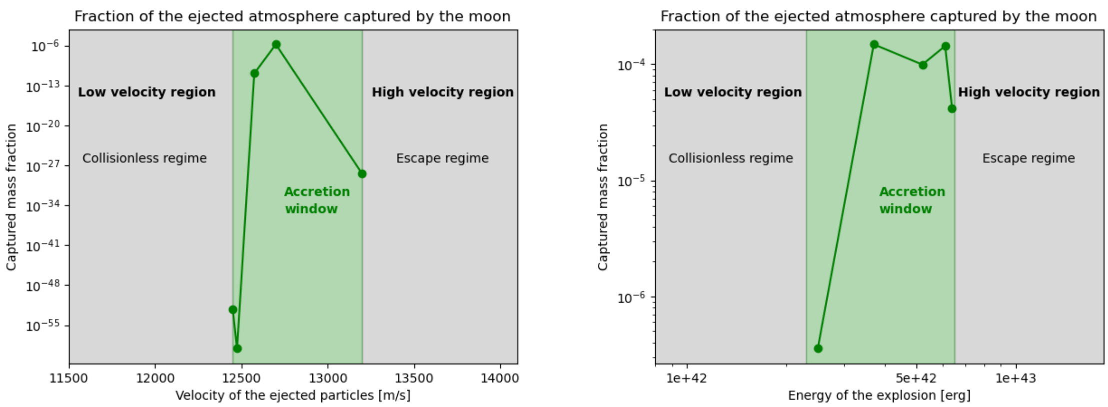

Figure 7: Left: results for Earth-moon like planet (manual simulation). Right: results for gas giant synthetic system (MESA simulation).

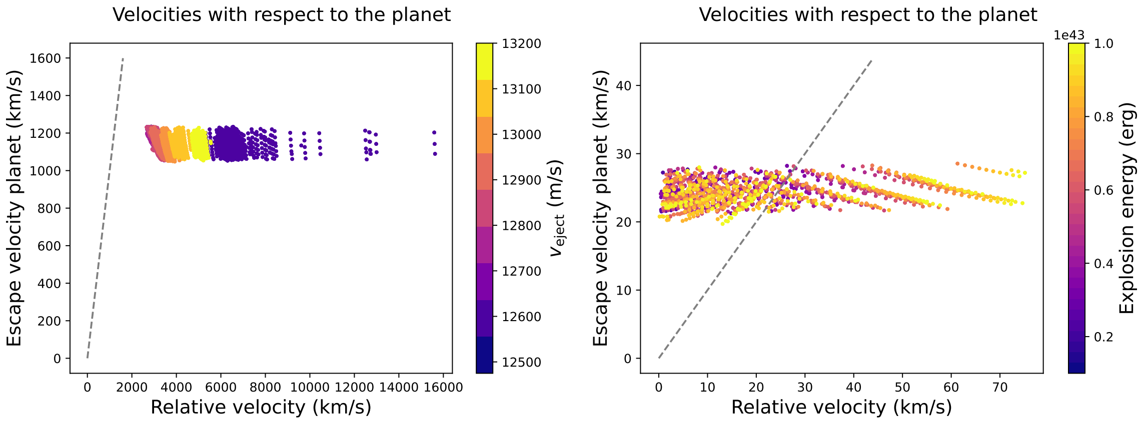

Figure 6: The left figure shows the relative velocity with respect to the planet and the escape velocity from the planet of the gas particles within the hill sphere of the moon at a certain time point in the simulation for the rocky planet. The right figure shows the same for the gas giant planet. The colours indicate the different ejecting velocities for the rocky planet and the injecting energies for the gas giant planet.

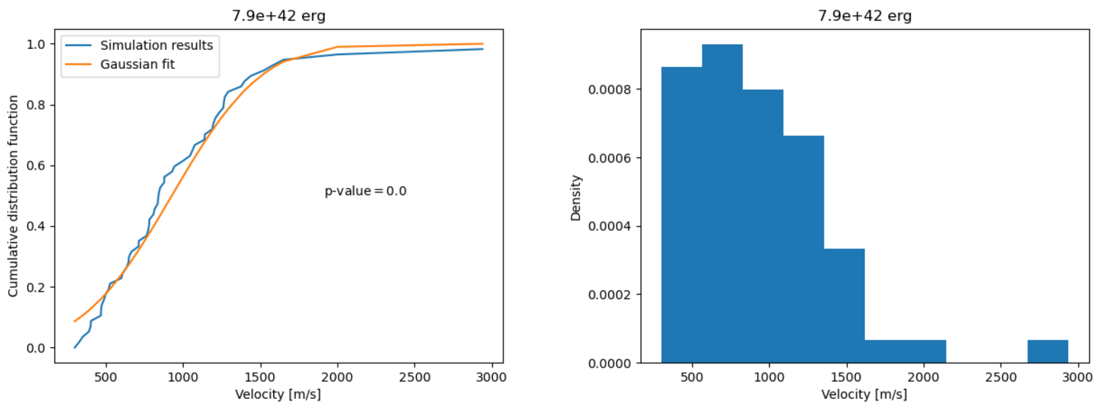

Figure 8: Example of what happens when the energy is too high: Gaussian fit fails because the left tail of the distribution disappears (no low velocity collisions).

4 Discussion

4.1 Physical interpretation

Accreted atmospheric fraction

Figure 7 shows the moon accretes a significantly lower fraction of the ejected material in the rocky system compared to the giant one. We interpret these results in terms of the M_{moon}/M_{planet} ratio. As given in equation (1), the Hill sphere radius increases with $(M_{moon}/M_{planet})^{1/3}$. A larger Hill sphere enhances the likelihood of a particle ending up bound to the planet. If we now look at Table 1, this ratio is almost 5 times larger for the giant system than for the rocky one. This explains the discrepancy between the accreted mass fractions. In the Solar System, M_{moon}/M_{planet} is higher for rocky planets, therefore we expect to find more planetary material on terrestrial moons. Another critical that should be studied in future works is the semi-major axis of the moon. Following the reasoning described above, we expect to find more accretion in more separated systems, as dictated by equation (1). In turn, the accretion window would move rightwards, as more energy is needed to transport the ejected particles further away from the planet.

Velocities in the hill sphere

In none of our simulations, we can actually measure an atmospheric particle being captivated by the moon and staying there for the rest of the simulation. However, we do measure for the rocky planet simulation one particle passing our bounding criteria as explained in Section 3.1 for a ejecting velocity of 12550 m/s. For the gas giant planet we find for both the simulation with an energy of 3.7×10^{42} erg and an energy of 4.0×10^{42} erg one particle that passes our criteria. These energies and the ejecting velocity do fall within the accretion windows displayed in Figure 7.

4.2 Caveats

Collisions

In this work, we have mostly focussed on the capture of a particle to the moon by being gravitationally bound. However, another method to get bound to the moon is by direct collision. In this scenario the (relative) velocity of the particle does not need to be as low as the earlier explored scenario. The number of collisions is then related to the radius of the moon and the distance between the planet and moon. To detect these collisions, we need a small timestep, smaller than the gas particle's crossing time of the moon. This crossing time, for a radius of 1800 km, which is the same order of magnitude as Jupiter's moon Io, would range, depending on the velocities of the gas particles, between 0.07 and 0.5 hours, which means our current timestep is too low to detect them. For the rocky planet we can do a similar calculation and find that the crossing time for a radius of $1R_{\oplus}$ ranges between 0.1 and 0.6 hours, which is also too small for our current timestep.

An estimate for the amount of collisions we expect in our simulations can be calculated by dividing the cross section of the moon by the cross section of the sphere that in which the orbit of the moon resides and will be of the order of magnitude of $R_{\text{moon}}^2/4a^2$ multiplied with the number of gas particles ejected from the atmosphere. For the gas planet, this is ~ 0.01 and for the rocky planet, this is ~ 1.6. We can conclude that we are likely missing the collisions for the rocky planet, but the resolution is too low for the gas giant to detect any collisions. However, we don't expect the amount of collisions to change with explosion energy, so those results can still be compared.

Resolution

As explained in the previous section, the amount of particles that would collide with the moon in our setup is not very big. To better track those, we would suggest a smaller timestep and a higher amount of SPH particles for future works. For measuring the amount of particles that is gravitationally bound to the moon we have both measured the velocities of the particles in the hill sphere of the moon and used a probabilistic approach to calculate this. The advantage of the probabilistic approach is that the resolution does not need to be large and the simulations can stay computationally inexpensive. However, we only detected at maximum one particle per simulation passing our criteria for being bound to the moon at one point in time. To be able to study this further the resolution should be higher.

Probabilistic approach

Here, we have given an order-of-magnitude estimate of the total accreted fraction by means of probabilistic arguments. However, this approach is not exempt of caveats. Specifically, it is not straightforward that the Gaussian fit holds for all the models. Although we tried to be rigorous by performing hypothesis testing and rejected the models with lowest p-value, the Gaussian approximation might still not be justified in some cases.

4.3 Future prospects

In view of the caveats of the probabilistic approach, future studies should focus on developing strategies to increase the resolution of the models, while avoiding prohibitive computing time. Additionally, more feasible scenarios should be explored, including localized explosions, planetary magnetic fields and realistic planetary systems. Finally, a large parameter study covering different planet and moon masses and orbital characteristics is also subject of a future work.

5 Conclusions

In this work we have studied the possibility that a moon captures part of the atmosphere of a planet in the event of an energetic explosion on the latter. First, we show two different ways of simulating planetary with AMUSE. One approach involves using MESA, and is more suited to giant planet. The second approach requires to construct an atmospheric profile manually, and it can handle both rocky and gas giant planets. Our simulations for a rocky planet and a gas giant planet show that atmospheric capture is possible for a narrow window of energies. Additionally, the mass fraction of accreted material increases with the ratio between the mass of the moon and the mass of the planet. More realistic simulations and larger parameter studies are needed to better understand the nature of this accretion window and its dependence with several planetary architectures.

References

Barnes, J., & Hut, P. 1986, Nature, 324, 446

Chen, H., & Rogers, L. A. 2016, The Astrophysical Journal, 831, 180

de Vries, N., Portegies Zwart, S., & Figueira, J. 2014, Monthly Notices of the Royal Astronomical Society, 438, 1909

Fulton, B. J., Petigura, E. A., Howard, A. W., et al. 2017, The Astrophyisical Journal, 154, 109

Glanz, H., Rozner, M., Perets, H. B., & Grishin, E. 2022a, The Astrophysical Journal, 931, 11

—. 2022b, , 931, 11

Hernquist, L., & Katz, N. 1989, , 70, 419

Nénon, Q., Poppe, A. R., Rahmati, A., & McFadden, J. P. 2021, Nature Geoscience, 14, 61–66

Paxton, B., Bildsten, L., Dotter, A., et al. 2011, , 192, 3

Pelupessy, F. I., & Portegies Zwart, S. 2013, MNRAS, 429, 895

Poppe, A. R., Fillingim, M. O., Halekas, J. S., Raeder, J., & Angelopoulos, V. 2016, Geophysical Research Letters, 43, 6749–6758

Portegies Zwart, S., McMillan, S., Harfst, S., et al. 2009, Nature Astronomy, 14, 369

Terada, K., Yokota, S., Saito, Y., et al. 2017, Nature Astronomy, 1, doi:10.1038/s41550-016-0026